Ann. N.Y. Acad. Sci. ISSN 0077-8923

ANNALS OF THE NEW YORK ACADEMY OF SCIENCES
Issue: *The Year in Cognitive Neuroscience*

# Concepts and principles in the analysis of brain networks

Gagan S. Wig,[1] Bradley L. Schlaggar,[1,2,3,4] and Steven E. Petersen[1,2,4,5]

Departments of [1]Neurology, [2]Radiology, [3]Pediatrics, and [4]Anatomy and Neurobiology, Washington University School of Medicine, St. Louis, Missouri, and [5]Department of Psychology, Washington University, St. Louis, Missouri

Address for correspondence: Gagan S. Wig, Department of Neurology, Washington University School of Medicine, 4525 Scott Avenue, Campus Box 8111, Room 2220, St. Louis, MO 63110. gwig@npg.wustl.edu

**The brain is a large-scale network, operating at multiple levels of information processing ranging from neurons, to local circuits, to systems of brain areas. Recent advances in the mathematics of graph theory have provided tools with which to study networks. These tools can be employed to understand how the brain's behavioral repertoire is mediated by the interactions of objects of information processing. Within the graph-theoretic framework, networks are defined by independent objects (nodes) and the relationships shared between them (edges). Importantly, the accurate incorporation of graph theory into the study of brain networks mandates careful consideration of the assumptions, constraints, and principles of both the mathematics and the underlying neurobiology. This review focuses on understanding these principles and how they guide what constitutes a brain network and its elements, specifically focusing on resting-state correlations in humans. We argue that approaches that fail to take the principles of graph theory into consideration and do not reflect the underlying neurobiological properties of the brain will likely mischaracterize brain network structure and function.**

**Keywords:** brain networks; graph theory; resting state functional connectivity

## Introduction

Numerous theoretical frameworks have guided the science of brain function. Until the 19th century, the predominant neuroscientific view held that cognitive processes were a product of the integrated functioning of the entirety of the brain and that the cerebral cortex was not composed of dissociable functional structures (i.e., cortical equipotentiality[1]). Several lines of evidence converged on a view of brain organization that emphasized localization of function whereby the cerebral cortex is composed of functionally distinct areas that mediate distinct processing operations. For example, examination of patients with focal brain damage (e.g., Refs. 2–4) revealed that lesions in specific locations produced specific deficits. The first known electrical stimulation studies of the cerebrum showed that electrical current delivered to certain brain regions, but not others, could reproducibly generate a motor response,[5] whereas Caton can be credited as being the first to make electrophysiological recordings from the brain.[6] Complementing these studies, detailed neuroanatomical investigation in the early 20th century revealed the differences in cytoarchitectonics across the cerebral cortex (e.g., Refs. 7 and 8), providing clear evidence of a nonhomogenous organization consistent with the notion of functionally discrete cortical areas. Observations obtained using more modern brain imaging hardware have largely supported the functional specialization point of view (e.g., Ref. 9). In fact, some neuroimaging researchers have argued that the cerebral cortex is composed, at least in part, of specialized areas that are dedicated to highly complex cognitive tasks or domains (e.g., thinking about others' thoughts; e.g., Ref. 10), a relatively extreme position on localization of function.

In parallel to observations providing evidence for cortical specialization, a separate body of work placed an emphasis on determining how information exchange between distinct areas may give rise to cognitive processing (e.g., Refs. 4 and 11). Initial support for the idea that brain connectivity mediates cognition was largely based on observations obtained in animal models and careful examination

doi: 10.1111/j.1749-6632.2010.05947.x



Ann. N.Y. Acad. Sci. 1224 (2011) 126–146 

of patient populations, wherein it was hypothesized that disrupted information exchange between brain areas could account for the behavioral disturbances that accompanied focal brain damage and psychiatric problems (for review, see Ref. 12). As a natural extension of these observations, typical cognitive functions such as attending to the outside world were considered to be a product of orchestrated interactions between multiple distributed brain areas that each mediated functionally specialized processing operations.

Brain science has largely maintained the viewpoint that cognitive processes are a product of the complex interactions between distributed objects of information processing.[13,14] This position has been greatly fueled by advances in the ability to quantify relationships between objects of interest. For example, modern brain imaging hardware and analysis techniques have enabled noninvasive measurement of the relationships shared between brain structures both in terms of evoked activity (e.g., effective connectivity[15,16]) as well as those that may reflect functional[17] (but also, see Ref. 18) or anatomical (for review, see Ref. 19) relationships not contingent on immediate task demands. Careful measurement of relations between brain structures has led to the concept that the brain is a large-scale network that is characterized by manifold connections and shared relationships.

Despite its seemingly unequivocal complexity, recent evidence suggests that the brain network, like numerous other systems, both man-made and biological, exhibits an underlying organization that characterizes and mediates its functions. A critical question is how does one go about untangling and making sense of this organized complexity? Numerous solutions have been offered. Although preliminary descriptions of brain networks have provided tantalizing descriptions of brain network architecture, it appears that there are almost as many diverging methods for conducting the analyses as there are publications on the topic (for recent reviews, see Refs. 20–22). Although we suspect that some choices of analysis and representation of networks may not significantly impact what is extracted from the underlying data, in the pages that follow we will argue that it is important that the decisions be guided by knowledge of fundamental principles relating to both the methodological approach (e.g., choice of analysis tools and models) and the nature of the network of interest (i.e., the brain).

We will largely focus our discussion and examples on the analysis of resting state functional connectivity MRI correlations (rs-fcMRI,[17,23] and for review, see Ref. 24), although many of the concepts and principles we invoke are equally applicable to the analysis of brain networks based on other types of relationships (e.g., structural, metabolic, electrical). rs-fcMRI correlations are defined by the temporal relationships of distinct brain areas observed in the absence of experimental demands. These relationships appear to mirror the distributed activity observed across a wide range of tasks and have been shown to be relatively reliable.[25–27] Accordingly, they offer a metric with which to quantify the strength of functional relationships between distributed brain areas.

To foreshadow the arguments to come, we take the position that any approach investigating brain network organization needs to simultaneously consider pairwise relations between the objects of interest, and that this goal is best achieved by the application of graph theory.[28,29] Furthermore, brain network analyses must also be grounded and constrained by assumptions and principles that are neurobiologically driven. To that end, we will argue that the current resolution limit of functional brain imaging constrains brain network descriptions to the level of cortical areas, and parcellations of subcortical nuclei at a similar level. A failure to strive to represent elements of the brain network accordingly would likely result in mischaracterization of the brain network itself.

## Networks and graph analysis

A network is a set of objects that interact or share some relationship with one another. Networks can be biological (e.g., social networks, ecological networks, and networks of protein–protein interactions) as well as nonbiological (e.g., communication networks such as the World Wide Web, electrical power grids, and air-transportation networks; for review, see Ref. 30). Accordingly, the science of networks tends to cross numerous, seemingly unrelated research disciplines and has applications ranging from controlling disease outbreaks to designing efficient urban centers. Critical in describing a network is that the objects, and the

relationships the objects share, can be formally identified and quantified in a meaningful way.

As the number of objects and relationships shared between these objects begins to increase in a given network of interest, it becomes increasingly difficult to represent the network in an efficient and organized way. Like numerous other researchers studying the science of networks, we advocate the adoption of graph theory, a branch of mathematics in which mathematical structures (graphs) are used to model pairwise relations between objects (for comprehensive introductions, see Refs. 28 and 29). The following section (1) reviews some basic principles of analyses using graph theory, including how simultaneously considering all pairwise relationships across objects in a network can be useful for understanding the structure and function of networks; and (2) outlines some of the current limitations of alternative approaches in the brain sciences.

Using graph theory, networks are most often described using one of two types of notations, but others are also possible and may be preferred depending on what information is to be represented. Each type of notation has its advantages, and each can typically be used to construct the others. Common across notations is the formal definition of the objects and their relationships. For present purposes, we will focus on the use of matrices and graphs to represent networks. A matrix of a network is typically referred to as an adjacency matrix, in which each $\text{cell}_{IJ}$ describes some relationship between object I and object J (Fig. 1A). Although matrices are a convenient way of efficiently representing a large amount of information, the network structure of numerous relationships can be difficult to visually apprehend when the matrix consists of more than a handful of objects and relationships. Graphs are abstract representations of the components of a network whereby objects are symbolized by nodes or *vertices* and the pairwise relationships shared between these objects are symbolized by edges or links (Fig. 1B). Although graphs do not completely ease the burden of deciphering network organization, they can be useful in visualizing important properties of the network's structure.

To illustrate the utility of graph theory for understanding the broader implications of considering pairwise relationships within a network, we will focus on two sets of properties that are frequently used to describe and understand network structure. For the purposes of this exercise, we will refer to the friendship network we have constructed in Figure 1. In this friendship network graph, nodes represent individuals in a fictitious social community, and edges represent mutual ties of friendship between the individuals. As one might expect, a real friendship network is typically much more complicated than the simple network depicted here. For example, social groups often include ties that are positive (friends) and negative (enemies, i.e., signed edges), can be in one direction or the other (i.e., directed edges) and have different strengths of relationships (i.e., weighted edges). Importantly, graph theory is well suited to incorporate many of these and other factors of interest. Nonetheless, we hope the reader will bear with our oversimplified model of a friendship network for purposes of illustration, as we will also be referring to details and concepts revealed from this model in subsequent sections.

The first set of graph properties we will highlight considers the position of an individual (node) in a network, and how this position can confer differing levels of "importance" of that individual toward information transfer and maintaining network integrity. Although individuals 7 and 13 each have six friends (or node degree 6), focusing on node degree misses the obvious role that individual seven assumes in the general integrity of the network. This individual's network position makes him/her an important conduit for information flow between relatively separate large groups of individuals (i.e., between the groups denoted by a blue and red underlay and the group denoted by a green underlay). Relatedly, if seven were removed from the network, the network would split the friendship network into two disconnected parts (assuming, of course, that additional friendship alliances were not formed in response to 7's actions). What this example highlights is a concept referred to as the *betweenness centrality* of a node: a measure that reflects the incidence with which a node occurs on many shortest paths between other nodes in the network. Interestingly, when considered according to this measure of betweenness centrality, individual 18 is more central than 13, despite the fact that individual 13 has more friends.

The second set of graph properties we will highlight considers the "clumping" of highly connected individuals into subgroups within a network. Returning to the friendship network example, if we

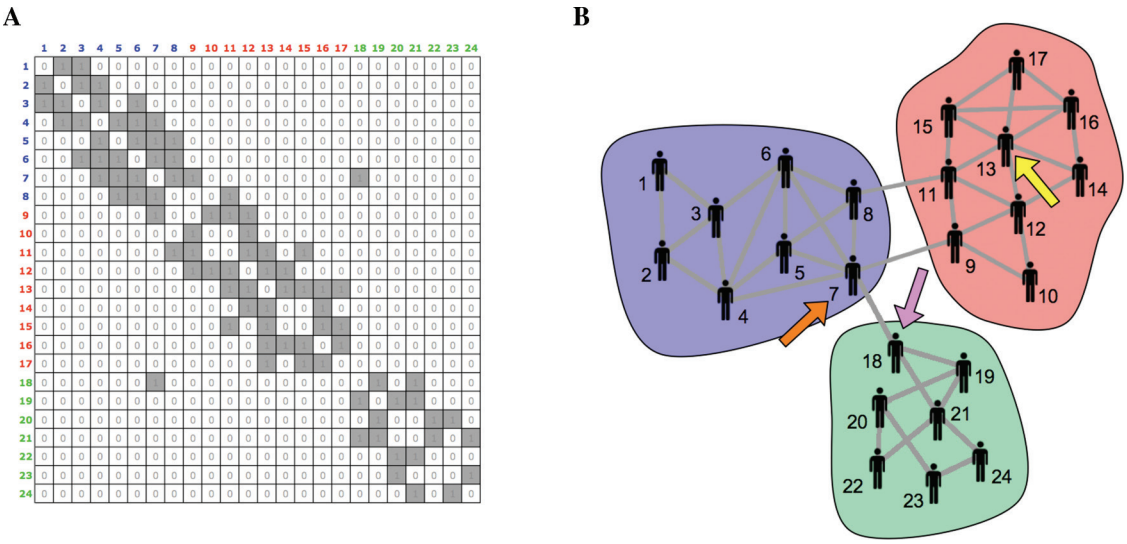


**Figure 1.** Two representations of a hypothetical friendship network. (A) Matrix representation of a social network. Elements (1–24) across the top row and down the leftmost column represent individuals. For every $cell_{IJ}$, the presence of a tie of friendship between the corresponding individuals I and J is denoted by a "1" and colored gray, whereas the absence of friendship is denoted by a "0." Individuals' labels are color-coded according to their corresponding community assignments in panel B. (B) Corresponding graph representation of the social network. Individuals are represented as nodes in the graph (stick figures); ties of friendship between the individuals are shown by the presence or absence of an edge connecting the two individuals. Color underlay denotes community assignments calculated using modularity optimization.[32] Using this method, communities reflect groups of nodes that are more connected with one another than would be expected by chance. Three communities were identified (blue, red, and green). Focusing on the nodes of the network reveals unique properties about the individuals. Some individuals can serve as high degree "hubs" for the network, as they have the highest number of relationships (i.e., 7 and 13, highlighted by orange and yellow arrows, respectively). An important relationship exists between individual 7 and individual 18 (pink arrow). If the relationship was severed, and no other ties were formed, the network would be divided into two unconnected components (blue and red community vs. green community). This property is captured by a node's betweenness centrality, the extent to which a given node lies on shortest paths in the network. Interestingly, individuals with high degree need not have high betweenness centrality, as is evident for individual 13, and individuals with low degree can rank high on betweenness centrality, as is evident for individual 18.

were to consider each of the friendship ties in isolation, we might assume that these ties were distributed somewhat randomly. We would miss the fact that the network contains a high incidence of clustering. In our social network example, quantification of this parameter would reflect the extent to which two individuals who are friends have other common friends. Relatedly, clustering can lead to subgroups of nodes that are richly connected to one another within the looser structure of the entire network. These subgroups are referred to as modules or communities that tend to reflect collections of nodes that share common features or functions, and several algorithms can be used to define membership quantitatively (e.g., Refs. 31–33). As is apparent, the fact that two nodes share a relationship does not mandate that they are in the same community, or even that they have any other relationships in common. All of these properties are only revealed when the pairwise ties of a network are considered simultaneously; we would have been oblivious to them if we had not considered all the friendship ties in the social network.

## Constructing a brain network

At its most complete depiction of reality, a representation of a brain network should include all the cortical and subcortical elements of information processing (nodes) and all the pairwise relationships shared between these elements (edges). For example, to generate a representation of an rs-fcMRI brain network, nodes should first be defined by parcellating the brain into meaningful objects of interest (e.g., brain areas). Building the adjacency matrix (i.e., defining the edges) then requires a quantification of the pairwise relationship between

each of the nodes in the network (e.g., the presence of a significant correlation between two area's resting-state timecourses).

It is important to realize the differences between an approach that utilizes graph theory to examine relationships within a network and some of the frequently used alternatives. One method commonly employed in rs-fcMRI studies is to generate a statistical map that represents correlation strength between a specific seed location and all other voxels in the brain (e.g., Refs. 17, 23, and 34). These maps reflect the strength of the relationship between each voxel in the brain and the seed, yet say nothing about how the identified voxels, or groups of voxels relate with one another or with any other group of voxels in the brain. In network terms, what are being identified are the neighbors of a particular node (i.e., the brain regions with which the seed region exhibits the presence of a relationship at rest); seed-based correlation maps are akin to identifying all the friends of an individual, without knowing anything about how those friends relate to one another or with other individuals of a social network. If we only defined the neighbors of node 7 in our friendship network (Fig. 1), we would fail to realize that these neighbors are actually parts of three different friendship communities.

To explicitly illustrate this preceding point, we conducted seed-based resting-state correlation analyses on a group of healthy young adults using a commonly employed preprocessing and analysis stream ($n = 52$; see Ref. 35 for details about participants, scanning, and preprocessing). The analysis was focused on the posterior cingulate cortex (pCC) of the "default network," a collection of brain regions that exhibit reliable patterns of task-induced deactivation during the performance of many goal directed tasks and are often correlated with one another during periods of rest[36,37] (for review, see Ref. 38). Resting-state timecourses were extracted from 5 mm radius spherical seed regions of interest (ROIs) generated around two previously published pCC peak coordinates identified from two different imaging methods (i.e., task-induced deactivations, MNI peak coordinates: 0 −45 42 [Ref. 39] and resting state correlations, MNI peak coordinates: −1 −34 38 [Ref. 34]. The correlation images of both seed regions were highly similar and revealed strong correlations with other regions of the default network (e.g., the angular gyrus and the ventromedial prefrontal cortex [vmPFC]). The left panel of Figure 2A depicts a conjunction of the two pCC correlation images, where the magnitude of the conjunction image reflects the average correlation across the independent pCC correlation images. The far left panel of Figure 2B depicts these same results in "pseudo-network" space, whereby the pCC has been placed in the center of the figure and a number of the regions identified in its correlation image are positioned around it (i.e., its neighbors). Although the pCC is related to each of its neighbors (by definition), it is not possible to know whether the neighbors themselves are related with one another without further analysis. To examine this possibility, resting-state timecourses were extracted from ROIs built around each of pCC's neighbors and pairwise correlations of all of these timecourses were computed to determine the presence of significant relationships ($P < 0.001$; middle panel of Fig. 2B). Although many of the pCC neighbors share a relationship, it is clear that there are a few exceptions (e.g., the anterior prefrontal cortex [aPFC] and the parahippocampal gyrus [PHG]). Accordingly, even among regions of the default network, the time course of regions correlated with the pCC need not be correlated with one another.

Curiously, in addition to regions typically associated with the default network, a number of other regions are correlated with the pCC as well, such as the dorso-lateral portions of the left and right middle frontal gyrus (MFG; Fig. 2A, left panel). Furthermore, the MFG also shares a relationship with other default regions (e.g., the angular gyrus; Fig. 2B, center panel). The MFG is typically implicated in operations related to control processes,[40,41] and does not typically exhibit task-induced deactivations.[37,42] In parallel, studies of resting-state correlations have frequently reported functional connectivity between the MFG and other frontoparietal control regions (e.g., Refs. 43–45). A likely possibility is that dissociable regions along the MFG exhibit heterogeneous processing operations. As such, the MFG region identified using our pCC seed may be distinct from the MFG regions that tends to correlate with control regions.

As a test of this hypothesis, we placed a seed in the right MFG identified in the pCC correlation image to examine its functional connectivity (MNI peak coordinates: 42, 24, 40; right panel of Fig. 2A). Although the correlation map reveals correlations

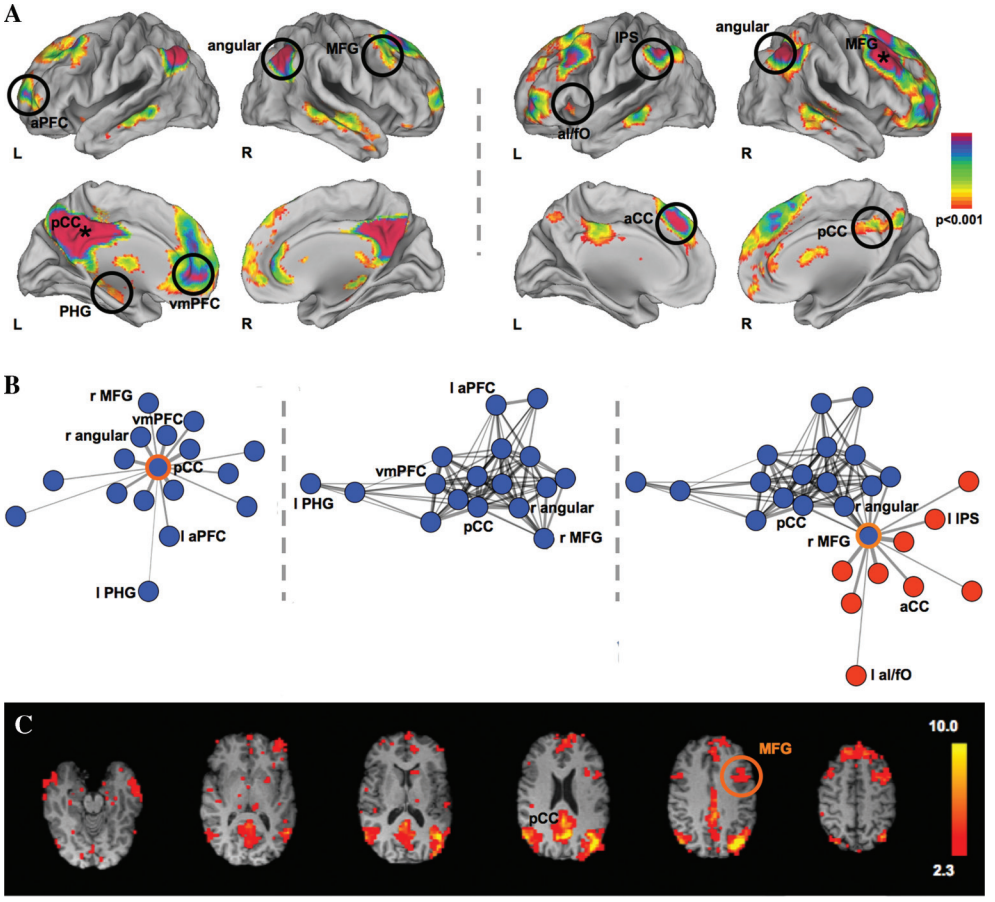


**Figure 2.** Seed- and ICA-based rs-fcMRI images fail to reveal the complete structure of pairwise relationships. (A) Statistical images on the left depict the results of a seed-based rs-fcMRI analysis. The pCC is strongly correlated with regions of the default network (e.g., vmPFC, angular gyrus) as well as other regions not typically linked to the default network (e.g., right MFG). The timecourse of right MFG was subsequently extracted to determine its seed-based correlations (statistical images on the right). The right MFG is strongly correlated with a number of default regions (e.g., pCC, angular gyrus) as well as regions that have been implicated in control processes (e.g., aCC, aI/fO, IPS), suggesting that while the two seed regions (pCC, MFG) are correlated at rest and share some common neighbors, they also exhibit different sets of relationships with other regions. (B) Depicts the rs-fcMRI analyses in graph space to illustrate how seed-based connectivity maps identify the nearest neighbors of the seed region. While the neighbors of the pCC (far left panel) are reliably connected with the seed ROI by definition, there is no information about the presence or absence of a relationship between the neighbors themselves. The middle panel depicts the significant relationships observed among the pCC neighbors (based on the correlations of their extracted timecourses). Although some neighbors of the pCC are correlated with one another (e.g., the vmPFC and left PHG), others' relationships are absent (e.g., the left aPFC and PHG). Notably, the right MFG region is correlated with other default regions as well (e.g., right angular gyrus). The rightmost panel includes the neighbors of the MFG that were identified by generating its seed-based correlation map as also depicted in the rightmost panel of (A). On its own, seed-based correlation images are unable to reveal the presence or absence of relationships amongst the seed's neighbors and with respect to other brain regions. Network space was visualized using a Kamada-Kawai algorithm implemented using the Social Network Image Animator software (SoNIA: http://www.stanford.edu/group/sonia/). (C) ICA identifies a "default" component that also includes the right MFG region, highlighting how independent components can also fail to reveal meaningful substructure both within and between components; ICA map adapted from Ref. 48.

with the pCC and other regions of the default network such as the angular gyrus (consistent with the pairwise correlations noted in the middle panel of Fig. 2B), many prominent correlations are present with regions linked to control including the inferior parietal sulcus (IPS), anterior insula/frontal operculum (aI/fO), and anterior cingulate cortex (aCC), suggesting that the MFG we have identified in the

pCC correlation map may indeed be a part of the same area frequently discussed in the context of control operations (right panel of Fig. 2B). To test further the possibility that the MFG region may exhibit distinct processing operations from that of pCC or any of the other default regions, we extracted the signal change of these regions from the task-evoked data set that was used to initially identify one of the pCC seeds (see Ref. 39 for details about experimental design and methods). This analysis revealed that during performance of an odd/even number judgment task, the pCC, in addition to many of the other typical default regions, exhibits deactivation relative to baseline (pCC: $t(44) = 7.69$, $P < 0.001$), whereas the MFG demonstrates a trend for increased activity relative to baseline ($t(44) = 1.75$, $P = 0.08$), providing evidence for a distinct processing role.

It should be apparent that simply examining a seed-based correlation image does not reveal how regions correlated with the seed are related to one another or with other brain regions, and that regions that subserve different processing operations and patterns of connectivity can be correlated with one another. Although we have not formally calculated the community assignments in this specific example (accurately doing so requires a more complete description of pairwise correlations between all brain regions, as outlined earlier), based on the results we have described it is possible that the pCC and MFG exist in different functional communities.

A second method that has been commonly used to identify patterns of correlation at rest employs a spatial-temporal decomposition of the resting-state time series using independent component analysis (ICA; e.g., Ref. 46). This multivariate approach separates resting-state BOLD signals into maximally statistically independent, spatial-temporal component maps. These components are then sorted into those that likely reflect components of noninterest or physiological noise, and those thought to be functional-anatomically important (often called *resting-state networks* [RSNs]). Although there are numerous methods for performing this last step, it is often done using some form of a template matching procedure where each component is compared to a set of "canonical" network maps (e.g., the default network). ICA has been used to identify numerous components thought to relate to sensory processing (e.g., vision, audition, motor, somatosensory), the "default mode," executive control, and visuo-spatial attention (e.g., Refs. 25, 26, and 47).

As with seed-based correlation maps, it is inappropriate to assume that an ICA-derived RSN is a distinct community of the network. The independent components reflect decompositions whereby each voxel in the component shares some temporal covariance with other voxels in that component. In this way, the information inherent in these components is different from the maps generated from seed-based correlations, which only reflect the relationship between each voxel and the seed region used to generate the statistical map. However, just as caution is warranted when assuming seed-based correlation maps reflect a community structure, so is the case for independent components. If ICA RSNs are the end stage of an analysis, the failure to assess the relationships between the substructure within a component and the relationships across components leaves the description of the network incomplete. At its best, it would be as if the three parts of the network in 1b were determined as groups of individuals, but all of the structure within a group and the relationships between the groups, were left out. As a familiar example, close inspection of a "default component" identified using ICA reveals inclusion of the MFG region highlighted earlier (Fig. 2C; Ref. 48).

The preceding set of comments is not to say that the information extracted by applying either of these methods (seed-based correlations, ICA) could not, in principle, be used for building a network adjacency matrix. Critically, however, doing so necessitates a fuller description of the pairwise relationships across putative brain areas followed by formal interrogation of these relationships using tools such as those within graph theory that are able to formally characterize network structure.

Although graph theory and its attendant tools provide an immensely powerful framework from which to study networks, the application to the study of brain networks is not straightforward. Most tellingly, the definition of the objects (nodes) of interest and the portrayal of the relationships (edges) between them raises a set of complex issues that are certainly not resolved at this point. Suboptimal representation of either of these elements can result in a distortion of important network properties.[49] We will next present our current ideas about these issues, attempting to address both the assumptions

of the tool as well as the inherent properties of the system of interest.

## Defining a node in a brain network

The nervous system functions as a large network of billions of independent processing elements (neurons), which are connected via axons spanning a total length of thousands of miles. A single neuron typically receives a large number of inputs from many other neurons, transforms this information, and then sends the processed information to many other connected neurons for further processing. Importantly, the patterns of anatomical and physiological relationships between neurons form specific patterns of spatial organization at multiple scales. In the cerebral cortex, for example, neurons form local circuits of computation. These circuits are often organized into larger units called columns that are about 1 mm in diameter. Functionally related columns form cortical areas roughly at the centimeter scale. Areas with similar functional properties and shared connections are then often grouped into functional systems. Each of these levels of organization could provide important objects of interest for network analysis.[50]

The advent of brain imaging has allowed noninvasive measurement of whole-brain anatomical features and correlates of neural physiology. Recent advances in imaging techniques have enabled rapid acquisition of large-scale data sets, which are amenable to the identification of many objects of interest as well as the anatomical or functional relationships shared between them. An important consideration when representing brain networks derived from brain imaging is the current resolution limit of the imaging tools, which enable the measurement of voxels that are typically cubes of a few millimeters. Accordingly, this spatial constraint limits brain network analysis to nodes above the millimeter scale, a limit appropriate to the scale of brain areas in the cortex, and nuclei or parcellations of certain nuclei in subcortical structures.

The challenge in defining brain nodes at this level lies in accurately identifying the appropriate boundaries to parcellate each of the unique areas, or nuclei, or subnuclei. Whereas individuals of a social network can be identified with relative ease, segmentation of cortical and subcortical structures into independent structures that exhibit dissociable information processing operations is a more formidable task. Unlike the map of the countries of the earth, which delineates geopolitical boundaries, brain science has yet to create a robust and reliable "brain map" that allows identification of each of the individual cortical areas, or subcortical parcellations. Nonetheless, neuroscientific studies of humans and other animals have provided ample evidence that the brain is composed of discrete and dissociable brain areas, and that these brain areas exhibit unique properties that allow them to be differentiated.

In the cortex, brain areas are characterized by properties related to both structure and function. These properties include architectonics (i.e., cyto-, chemo-, and myeloarchitectonics), patterns of common or dominating interareal connectivity, physiological characteristics (inferred from single and multiunit recording, analysis of deficits following focal lesion, and functional neuroimaging), and topographic organization.[51,52] As an example, each of these properties can serve to distinguish primary visual area V1 from area V2. The cortical columns of V2 can be easily differentiated from those of V1 by a presence of large pyramidal neurons in layer III of the former and a cell-poor sublamina IVb in the latter.[7] LGN input to V1 is evidenced by the stria of Gennari, a stripe of myelinated axons that terminates in layer IV of V1 gray matter (e.g., Refs. 53 and 54). Along these lines, examining patterns of interareal connectivity reveals that both areas exhibit similar patterns of direct reciprocal connectivity with a collection of visually responsive areas; however, a number of differences exist that allow differentiation such as the connectivity with ventral intraparietal area (VIP), which is strong for V2 but not V1 in the macaque cortex.[51] Functionally, although both V1 and V2 contain neurons that are selective for stimulus orientation, spatial frequency, length, direction, and binocular disparity,[55–60] V2 neurons exhibit larger receptive field sizes and sensitivity to more complex visual properties such as subjective contours.[61,62] Furthermore, a complete map of retinotopic space is recapitulated in each of the two visual areas providing further support of distinct processing operations on visual input. Importantly, a similar approach as that highlighted in our example has been used to identify brain areas within sensory (e.g., auditory,[63] somatosensory, and motor[51]) as well as "association" cortex (e.g., frontal

cortex[64,65]), suggesting that areas are an organizing principle throughout the brain.

Given that many of the techniques used in the animal studies are not easily available for living humans, how does one use noninvasive imaging to identify brain areas for the purposes of node definition? As is the case for defining areas in animals, it is likely that no single approach will arrive at a complete and robust description of brain areas in humans, and methods for identifying these parcels are in early stages. Ultimately, as in animal studies, this goal will likely be achieved by mutually informative evidence provided by numerous techniques and modalities,[66] that converge on a consensus set of areas. At present, we advocate approaches that leverage the availability of large-scale data sets to identify consistent "hot spots" of task-evoked activity as well as techniques that are able to parcellate brain areas based on patterns of connectivity or clustering.

One approach for constructing a large-scale "areal" node set involves searching across large collections of task-evoked fMRI studies to localize brain activity circumscribed to distinct brain regions (i.e., finding peaks or "hot spots") and then building regions around these hot spots (e.g., spheres). The logic here is that the hot spots represent epicenters of activity within areas that likely mediate dissociable and functionally meaningful information processing operations. Utilizing the large databases that have aggregated peak coordinates of activation across many studies (e.g., Brainmap [http://brainmap.org], SumsDB [http://sumsdb.wustl.edu]) can facilitate this process. An obvious limitation to this approach is that it is restricted by the availability and breadth of imaging studies that sample across a fixed number of stimulus sets and task manipulations. Second, although regions can be built around the hot spot of a putative area for the purposes of node representation, this does not mandate that the region has captured the "behavior" of the brain area in its entirety. Building regions around reliable peaks of activation will likely fail to include information from area boundaries. By assuming a constant size fixed around a peak, using functional regions to define nodes may result in a misrepresentation of the true relationship strength between brain areas.

A second technique is to look for abrupt transitions in whole-brain patterns of either anatomical or functional connectivity across voxels, and then translate these transitions into boundaries between cortical areas. The logic here is that a collection of voxels belonging to a single area should demonstrate similar patterns of relationships, and that these patterns should be dissimilar between adjacent brain areas. This method of area identification has been accomplished for limited stretches of cortex by tracking changes in DTI tractography[67,68] as well as patterns of resting state correlations.[69]

It is important to validate that the boundaries identified using patterns of connectivity reveal meaningful functional divisions. A recent study by Nelson *et al.* applied the boundary detection analysis with rs-fcMRI across a grid situated on the surface of the left lateral parietal cortex (LLPC) in humans[70] (Fig. 3A). Following identification of putative areas based on their patterns of resting-state correlation, graph analysis was used in conjunction with resting-state connectivity to determine whether the peak regions within these putative areas might be situated within different functional communities. Community detection revealed the presence of six distinct functional communities within the LLPC. Importantly, the divisions were independently confirmed by examining profiles of evoked timecourses during the performance of tasks related to memory retrieval (Fig. 3B). Additional support for similar divisions in this part of the brain in humans has come from examining profiles of connectivity across alternative brain imaging modalities (i.e., connectivity of rs-fcMRI and DTI tractography[71] as motivated by divisions that were identified in probabilistic cytoarchitectonic maps[72,73]). Consistent with these latter findings, the divisions noted by Nelson and colleagues demonstrate striking correspondence with the same cytoarchitectonic divisions (Fig. 3C). Notably, a much earlier cytoarchitectonic parcellation scheme by Brodmann[7] does less well at identifying the unique divisions (Fig. 3D).

In addition to boundary definition, a number of other complementary methods may also be able to provide a brain area parcellation using rs-fcMRI. Some of these include clustering analysis of voxels based on correlation pattern similarity,[74] local connectivity,[75] and shared spatio-temporal covariance (e.g., ICA; Ref. 46). Furthermore, some of these tools may also be well suited to delineating parcellations of subcortical structures (e.g., Refs. 76 and 77). Because of the hierarchical nature of brain organization (e.g., Ref. 51), diligence is required in employing

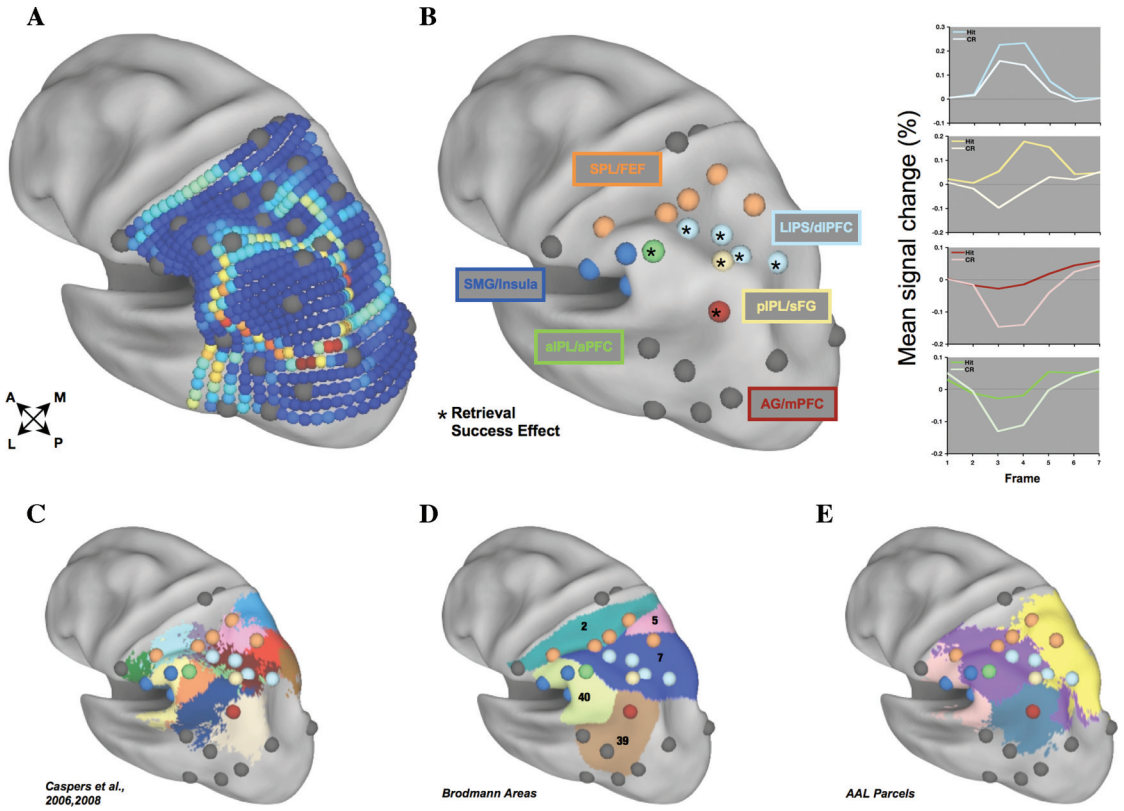


**Figure 3.** Putative brain areas of the left lateral parietal cortex defined by rs-fcMRI boundary mapping and correspondence with anatomically defined cortical parcels. (A) Colored underlay represents the results of probabilistic rs-fcMRI boundary mapping of the left lateral parietal cortex (LLPC) of healthy young adults. "Cooler" colors represent stable rs-fcMRI patterns (i.e., point-to-point similarity in the pattern of correlation maps), whereas "hotter" colors represent high border likelihood based on rapidly changing rs-fcMRI patterns (i.e., point-to-point differences in the pattern of correlation maps). Grey spheres denote the peaks of stability within each of the putative cortical areas generated from the rs-fcMRI boundary-mapping image. (B) The LLPC peaks identified from boundary mapping are named and color coded according to their community membership based on patterns of rs-fcMRI connectivity. Importantly, regions of the distinct communities exhibit dissociable patterns of functional activation during memory retrieval tasks. Asterisks denote peaks that exhibited memory retrieval effects (hits greater than correct rejections; see panel to the right) across a series of studies. Panels A and B adapted and modified from Ref. 70. (C) A recent cytoarchitectonic division based on postmortem examination of 10 human brains [72,73] is painted on as an underlay and reveals relatively good correspondence with LLPC peaks defined from rs-fcMRI boundary mapping. Although some differences still exist (e.g., no rs-fcMRI peaks were found in the dark blue cytoarchitectonic parcel), the cytoarchitectonic parcellation offers greater specificity than an earlier one provided by Brodmann (D). (E) Depicts the same LLPC peaks overlaid on parcels defined by morphological landmarks (i.e., gyral and sulcal boundaries using automated anatomical labeling (AAL)[80]) to demonstrate rather poor correspondence with the putative rs-fcMRI divisions. For example, the parcel shaded in purple includes many regions that are part of distinct functional communities.

many of these methods to ensure that the clusters represent, as best as possible, individual areas and not adjacent areas with similar properties or connectivity, or worse yet, collections of distributed areas that are actually neighbors of one another or a community within the network.

Three additional limitations, pertaining to techniques that strive to identify areas via transitions in connectivity or clustering, are worth considering. First, the arbitrary nature of the spatial positioning of voxels during data acquisition may preclude delineation of sharp boundaries. Second, spatial registration of area boundaries across participants is likely to be difficult in practice. Third, nodes that represent areas will inherently differ from one another in terms of their physical size. As larger areas are composed of a greater number of voxels, and signal variance will scale with the number of

voxels that contribute to its estimate, quantification of pairwise relationships may be disproportionately more reliable for larger brain areas.

As a practical solution, ROIs can be built around the peaks or centers of putative areas that have been identified using transitions in connectivity or clustering, such that voxels at the boundaries are excluded. This approach helps to minimize the likelihood that the node inadvertently crosses an area's boundaries both within and between participants. Building fixed size regions (e.g., spheres) around the peaks or centers of putative areas has similar benefits and also alleviates some of the problems pertaining to differences in signal variance that will accompany interrogation of nodes that represent areas of different sizes.

As there is presently no complete description of a brain area parcellation, there have been several additional proposed solutions for defining brain nodes for the purpose of network analysis. These solutions typically provide a full parcellation of the brain, but many of these solutions do not specifically strive toward mapping area distinctions. The trade-off between using a partial brain area parcellation that is constrained by neurobiology and a full parcellation that is not subject to the constraints has, in our opinion, led to numerous discrepancies both in terms of how investigators have chosen to label a "node" and in terms of what the analyses of these networks reveal.

A commonly used brain parcellation technique identifies gyral and sulcal boundaries to segment the brain into morphologic parcels (e.g., Refs. 78–80). These parcels have been used as brain nodes across a series of brain network studies. In addition to the considerable variation that is present across macroscopic surface features that limit the extent to which a given parcellation can be applied across subjects (e.g., Ref. 81), it is important not to confuse these anatomic parcels with actual cortical areas. Functional areas need not obey the divisions created by parcellation techniques based on anatomical landmarks. A functional area can span across a morphological boundary and multiple areas may be present within a single morphologically defined parcel. The localization of area V1 described earlier serves as a prominent example for both of these points. Area V1 in human and many nonhuman primates spans the calcarine sulcus, occupying its upper and lower folds (although it should be pointed out that this feature is accommodated in a few of the anatomically based parcellation schemes[82,83]). In turn, the crown of the outward folds also maintains the representation of the adjacently placed area V2 such that the V1/V2 border is delineated by features that are independent of their copresence on a gyral fold, as outlined earlier. Consistent with these preceding arguments, focusing on the putative parietal divisions outlined earlier reveals that multiple regions may be represented within a single anatomical parcel, and single areas may span multiple parcels (Fig. 3E).

One potential solution to avoiding coarse anatomical parcels that may aggregate distinct areas has been to subdivide the large parcels into smaller, equally sized chunks using regular or random segmentation. Although this approach acknowledges the heterogeneity of areas that is present within the larger parcels, its limitations should be quickly apparent (in addition to ignoring the fact that anatomic parcellation may divide brain areas at the outset). First, without an idea of how many areas should actually exist within a parcel, how does one decide how many smaller chunks should be created? Second, even if the quantity of areas was known, this does not solve the problem of deducing their shape or spatial arrangement. Brain areas vary in shape and size, producing formidable limitations to the approach. Within the human visual cortex, for example, the size of V1 can be up to twice the size of V3 and need not correlate across individuals.[84] These differences are substantially more pronounced when comparing across other areas.[7,85] Finally, segmentation of anatomical parcels into smaller chunks introduces similar problems as that which is created with anatomical parcellation itself: inappropriately dividing true areas and potentially aggregating numerous areas into a single chunk. Within the lateral parietal cortex for example, without a prior knowledge of the landscape of area boundaries (Fig. 3A), segmentation is likely to incorrectly divide areas.

Conceptually similar to the random segmentation of coarse anatomical nodes, another method of defining nodes has been to parcellate the brain at the finest spatial resolution possible: at the size of units of signal acquisition (i.e., voxels). Accordingly, the likelihood with which a node contains multiple distinct brain areas is minimized. Although interrogating voxels is suitable in the statistical analysis of brain images when the goal is to identify

clusters of voxels with similar properties (e.g., evoked activity, connectivity), treating a voxel as a node in a network explicitly implies that it is being modeled as a distinct unit of information processing. The theoretical problem should be clear. Furthermore, modeling voxels as nodes also has practical implications that will distort brain network measures. Given that we are limited to the level of areas with brain imaging, it is important to remember that brain areas vary in size relative to one another.[7] For example, size difference can be more than 33 fold among visually responsive areas (e.g., V1 vs. MT; see Ref. 83). As all voxels existing within a functional area will undoubtedly share an edge with one another, graph measures that focus on specific properties of nodes will be biased toward nodes (voxels) existing within areas (and possibly communities) that are larger than others, and measures describing global properties of the graph will be distorted due to a misrepresentation of areas as a function of the number of voxels they contain.

A number of investigators have begun to explore how differences in node definition can affect network properties. The results serve as a strong empirical demonstration of some of the caveats of node definition we have highlighted. Along with the deviation from the known organizational principles of the brain, if the analysis was not sensitive to the problems and constraints of area parcellation we have outlined, then it is possible that the multiple approaches for defining a node might converge on similar results and patterns. However, differences in node definition using a number of the methods outlined above (anatomic parcels, random divisions of anatomic parcels, voxels) produce large quantitative and qualitative differences on measures of both anatomical[86] and functional[87–89] brain networks. Global network measures including those quantifying the size of the most connected component, clustering coefficient, path length, mathematical fit of the degree distribution to a specific function (e.g., a power law), and efficiency all vary greatly across the methods of node definition (e.g., see Table 1 of Ref. 88). For example, depending on the sampling procedure used, measures of "small-worldness" ($\sigma$) can deviate by more than 28-fold (compare $\sigma_{AAL}$ [82 anatomically defined nodes] versus $\sigma_{4000}$ [randomly parcellated nodes constrained by AAL parcels] in Ref. 86; Figs. 4A and B). Similarly, network metrics focusing on the behavior of individual nodes also differ across the methods. For example, the identification of the node with highest degree (i.e., degree centrality) can depend on the method of node definition used (Fig. 4C). While qualitative differences may be related to resolution limit in some cases, we argue that a considerable portion of the deviation is likely due to the behavior of nodes that are defined by methods that are incompatible with one another and, more importantly, do not represent the underlying organization of the brain.

We refer to the geopolitical map of the world to serve as a final illustration of some of the caveats to defining nodes by coarse and/or arbitrary parcellation schemes (Fig. 5). If the aim were to build a network in which the nodes represented the countries of the world (Fig. 5A), parcellation based on coarse morphological features such as boundaries of land and water (Fig. 5B), random division of parcels into similarly sized chunks (Fig. 5C), or uniform division wherein nodes were represented by pixels (Fig. 5D) would all result in serious mischaracterization of the boundaries of countries. As a parallel, the problem with applying similar approaches for defining brain areas that have distinct properties and potentially detectable boundaries should be evident.

## Defining an edge in a brain network

In a graph, an edge represents the pairwise relationship or interaction between two independent nodes. The resolution limit of brain imaging imposes similar constraints on edge definition as that of nodes, wherein the modeled relationships must represent either functional or anatomical connections between brain areas. We have principally focused our discussion on measures of rs-fcMRI whereby timecourses of activity are typically extracted from BOLD volumes that are collected while participants are lying in the scanner passively fixating a crosshair. rs-fcMRI most often focuses on patterns of low-frequency (<0.1 Hz) BOLD signal fluctuations obtained during periods of rest and has been linked to neuronal low-frequency potentials in humans.[90,91] Furthermore, rs-fcMRI signals are inherently graded as they reflect the magnitude of strength of correlation between voxels or brain regions.

Although the collection of resting-state time series is relatively straightforward and can be performed across different cohorts of individuals in the absence of performance confounds, a number

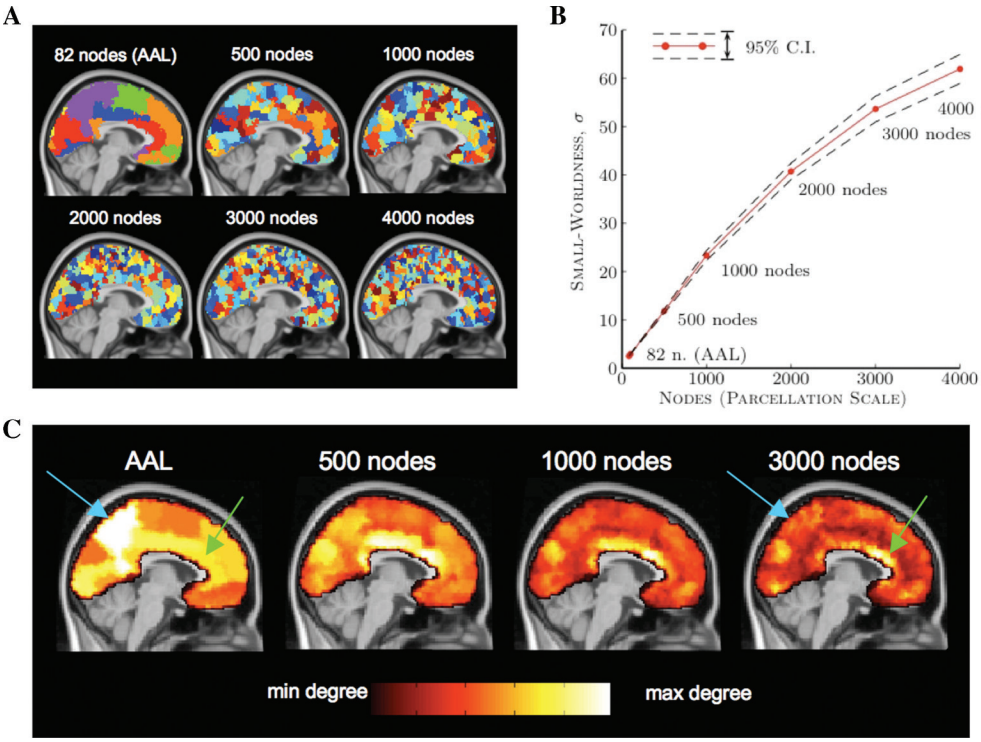


**Figure 4.** **Brain area parcellation using anatomical borders or arbitrary divisions results in variable network metrics and node properties. (A) Depicts six independent node parcellations including anatomical definition based on sulcal and gyral boundaries (AAL[80]) and subparcellation of these anatomic parcels using an algorithm that randomly divides nodes to produce nodes of smaller scale. (B) Depicts the quantification of network efficiency by way of a small-world metric[136] across the different parcellation scales. *Small worldness* ($\sigma$) is defined as the ratio of a network's clustering coefficient (normalized by a comparable random networks clustering coefficient) relative to the network's average path length (normalized by a comparable random networks average path length[137]). As evident in the graph, the value of $\sigma$ can differ up to 28-fold depending on the node parcellation scale (compare 82 node AAL to 4000 node). This variability is largely driven by differences in the clustering coefficient (not shown) across the node sets. (C) Depicts midsagittal slices of four of the node sets, with each node color coded according to its degree (number of connections) within the network. The variability of node properties across parcellation scales is readily apparent. The nodes with highest degree vary across the four node sets. Although the brain network using AAL parcellation identifies a node situated within the medial parietal cortex as being the most connected (blue arrow), a region in anterior cingulate cortex is identified as being most connected in the 3000 node set (green arrow). Connections were measured using DTI tractography. Figures adapted and modified from Ref. 86.**

of important issues in the analysis and interpretation of these signals merits consideration. We recognize that edge representation will surely evolve in parallel to the development of more sophisticated analysis techniques and a deeper understanding of the underlying source of the signals. At present, the approach we and many others have adopted and described herein is relatively conservative. First, each node's resting state timecourse is extracted from a given subject and preprocessed for removal of physiological sources of noise. Second, pairwise correlations between the timecourses of each node pair are calculated to quantify the strength of relationships. Finally, weighted adjacency matrices, whereby edge weights are retained and reflect the strengths of correlations between nodes are constructed and sparsified according to a desired statistical or edge-density threshold.

Several alternative choices may be made to estimate the strength of functional relationships. For example, pairwise relationships may be quantified according to spectral coherence (e.g., Ref. 92), correlations of wavelets derived from the variance decomposition of the resting-state time series,[93] or measurements that estimate directional information flow[94] (importantly, the sluggish nature of the

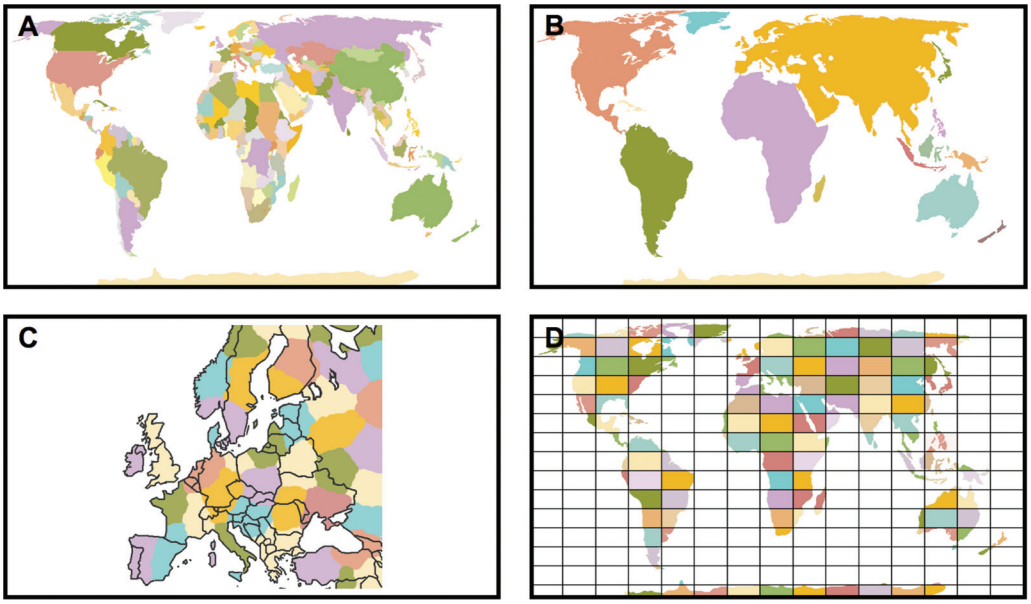


**Figure 5.** Coarse or arbitrary node parcellation can result in inaccuracies when building a network to represent the relationships between countries of the world. (A) Map of the world's countries (published in 2002). (B) Depicts a schematic in which areas are divided according to large morphological features of the planet (i.e., boundaries between land and water). Although some countries are accurately identified (e.g., Australia), this coarse parcellation scheme largely results in the aggregation of countries with distinct and independent relationships (e.g., all countries within Europe and Asia are combined into a single large area). (C) Focuses on a more recent depiction of the European subcontinent to demonstrate that randomly dividing coarse parcels into smaller chunks to potentially account for nonuniformity can fail to accurately represent divisions. If no prior knowledge is brought to the parcellation, single countries can be divided across multiple nodes (e.g., France), and a single node can contain multiple countries (e.g., the purple node in the center spans the Czech Republic, Poland, Slovakia, and Hungary). (D) Similarly, arbitrarily dividing the map based on a randomly placed grid of pixels can result in gross mischaracterization of countries. Large countries (e.g., Canada, Russia, and United States) are split into multiple independent nodes, which could distort network metrics aimed at describing the organization and behavior of countries in the world. Furthermore, this random division also misrepresents most geopolitical boundaries.

BOLD response coupled with the temporal resolution of functional imaging likely makes this latter option quite difficult). As an alternative to using the full correlation between a pair of nodes as a measure of strength of relationships, some researchers have begun to examine whether a partial correlation that has regressed out the variance of other nodes that may be mediating the relationship may be better suited to defining pairwise functional relationships (e.g., Ref. 95). Although simultaneously partialling out variance from a large number of variables can result in mathematical irregularities that distort the underlying data, further developments of this approach may provide a robust way of estimating the strength of more direct functional relationships.

One version of partial regression that has often been used as a form of preprocessing involves regression of the mean global brain signal from each voxel prior to extraction of the time series (e.g., Ref. 34). A consequence of this processing step is that the correlations get distributed around a mean value of "0," producing strong positive and negative correlations. As such, there has been a debate about the validity and interpretation of the approach and the observed negative correlations.[96,97] The regression step mathematically mandates that the correlations are distributed around the mean global signal. Accordingly, although caution is certainly warranted when interpreting the influence of one region over another based on the correlation of their timecourses, it is fine to interpret the correlations as reflecting covariance relative to the mean signal as opposed to spurious artifacts that are epiphenomenal consequences of the mathematical pipeline.

Are negative correlations biologically meaningful? Preliminary evidence suggests that they are.

Negative correlations exhibit a distinct spatial structure, are consistent across subjects, and recent studies have demonstrated that they are present even when the mean signal is left in (e.g., Ref. 98). Furthermore, antagonistic relationships are expressed throughout neurobiological circuitry and these relationships have a direct impact on function. For example, the caudate/putamen's inhibitory projections onto the external capsule of the globus pallidus within the circuitry of the basal ganglia[99] or the inhibitory projections from the substantia nigra pars reticulata on the superior colliculus[100] are fundamental to the functioning of those systems. Future work will be needed to determine the correspondence between circuit inhibition, negative correlations, and their influence on network structure.

Although many network edges are easy to define and can be represented by the presence or absence of the relationship of interest (e.g., whether or not two stations are connected to one another in a railway transportation network), many other edges are more "fuzzy" such that a simple binary distinction can be misleading. Relationships between brain areas exhibit this latter property, whereby the strength of relationships (functional or anatomical) between nodes is inherently variable or weighted. Caution is warranted when constructing graphs that discard the weight of the relationship measure (i.e., creating an unweighted network), as reducing relationships to binary distinctions results in losing important information about differences in the strength of the relationships across pairs. Care must also be taken when thresholding an adjacency matrix to remove edges. Although thresholding can remove weak relationships that may not be physiologically relevant, excessive thresholding for the purposes of computing graph properties or constructing comparable graphs across subjects or cohorts can result in the creation of a matrix that, while sparse, misrepresents the underlying connectivity. Edge weights likely reflect neurobiologically relevant properties of brain organization. Variability across measured relationships may reflect differences in the nature, strength, density, or probability of detecting a relationship. Efforts to quantify brain networks should keep these issues in mind, as thresholding and dichotomization can obscure important properties and alter the characterization of the resulting brain network.

To conclude this section, we turn to a discussion of the source of rs-fcMRI signals. Are functional relationships obtained from rs-fcMRI equivalent to the anatomical relationships that are identified by measurement of fiber bundles using diffusion imaging? A number of studies have attempted to directly address this question (for reviews, see Refs. 101 and 102). A high degree of correspondence has, in some cases, been observed between measurements of functional and anatomical connectivity. Comparisons have ranged from those focusing on regions on adjacent gyri,[103] to distributed regions sampled from a subset of interest,[104] to the whole brain.[105–107] Together, these studies provide strong evidence that functional relationships obtained using rs-fcMRI are likely constrained by the underlying anatomical architecture. Consistent with these findings, investigation of patients with agenesis of the corpus callosum due to congenital defect,[108] or following complete resection of the corpus callosum for treatment of intractable epilepsy[109] have noted weaker interhemispheric functional correlations relative to intrahemispheric correlations suggesting that a portion of the interhemispheric connectivity is mediated by callosal fiber passages (but also see Ref. 110).

Importantly, although areas that share a direct anatomical connection between one another typically exhibit a significant resting-state functional correlation, the reverse need not be true. An example of this comes from an investigation of the macaque monkey where the functional correlation structure of visually responsive regions reveals subareal, retinotopic organization.[111] Despite the absence of direct interhemispheric connections involving V1 away from the horizontal meridian,[112] correlations between bilateral representations of the peripheral visual field in V1 (e.g., along the eccentric portions of the horizontal meridian) are stronger than the correlation between the peripheral and foveal representations within one hemisphere (Fig. 6). This suggests that the observed correlations may be sustained by an indirect pathway that respects visual retinotopy along the eccentricity axis (e.g., via dorsal MT). Consistent with this, the aforementioned study of human connectivity by Greicius *et al.*[104] noted an absence of direct anatomical connectivity between the vmPFC and medial temporal regions (as assessed using DTI tractography) despite the presence of significant functional correlations between these regions, suggesting that the relationship may be mediated by connectivity via an intermediate region (e.g., pCC). These and other

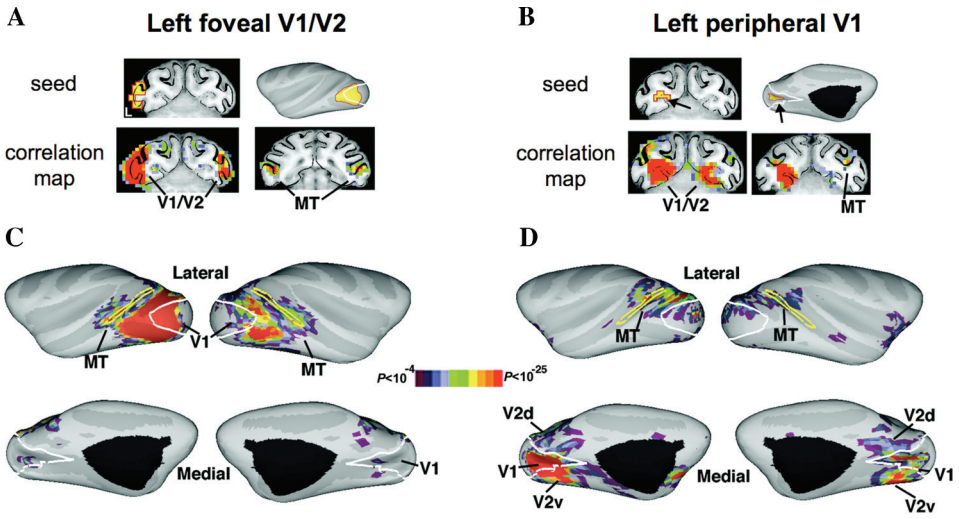


**Figure 6.** Resting state correlations identify relationships between regions that do not share a direct anatomical connection. Maps depict the results of a seed-based rs-fcMRI study in the Macaque. (A) The time course of a seed region placed in the left foveal representation of V1/V2 is strongly correlated with the foveal representation of bilateral MT and contralateral V1/V2. Notably, correlation with the peripheral representation of V1 is lacking. (B) The time course of a seed region placed in the left peripheral representation of V1 is strongly correlated with the peripheral representation of bilateral MT and contralateral V1. This functional connectivity is present despite a lack of a direct anatomical connection between peripheral representations of V1 across the two hemispheres. Panels (C) and (D) depict the same correlation maps on inflated cortical surfaces for foveal and peripheral seed regions, respectively. Together, these results provide evidence that resting-state correlations that respect visual retinotopy along the eccentricity axis may be sustained by indirect pathways. Figures adapted and modified from Ref. 111.

results have all converged on the principle that patterns of rs-fcMRI do not represent a 1:1 correspondence with direct anatomical connectivity (where anatomical connectivity is defined by the observed presence of a fiber bundle). In line with these observations, incorporating indirect anatomical connections (i.e., those that mediate area-to-area connectivity via two steps) can account for a further portion of the variance observed in functional correlations across numerous brain regions.[106]

If not exclusively a measure of direct anatomical connectivity, what do functional relationships reflect and how are they established? One possibility is that they reveal a form of unconstrained cognition (i.e., "thinking") present while subjects are resting in the scanner. However, numerous pieces of evidence suggest otherwise. The strongest of these are based on the observation that the distributed patterns of correlation are relatively stable across multiple states of alertness in addition to resting wakefulness including periods of sleep (e.g., Refs. 113 and 114), anesthesia (e.g., Ref. 115), and during task performance (e.g., Ref. 116). Furthermore, given the nature of the signal on which rs-fcMRI correlations are based, if the low-frequency correlations are indicative of actively "thinking," one would have to posit that these processes are occurring at a frequency of at least once every 10 s (i.e., approximately 0.01 Hz). Curiously, a portion of rs-fcMRI correlation variance may be effected by task demands, imposing practical constraints on the collection and analysis of rs-fcMRI (e.g., Refs. 117 and 118), but also providing preliminary evidence that low-frequency signals may have an impact on immediate behaviors, or vice versa.[119–121]

An alternative possibility, one that we favor presently, is that the low-frequency relationships evident between brain areas during periods of rest reflect a signature of coactivation that has been sculpted over time. Resting-state relationships may be mediated by a "Hebbian-like" mechanism in which the continual recruitment of a set of areas for a common purpose results in changes in the synaptic efficiencies between them. Low-frequency temporal synchrony may be a manifestation of these changes and ultimately provide a medium for more

efficient information transfer when the areas are subsequently recruited for specific task demands.

Convergent data provide evidence for this hypothesis. First, patterns of resting-state correlations largely mirror the spatial distributions observed in the context of task-evoked activity (e.g., Ref. 122). Second, resting-state relationships can be modified in a relatively short time frame (i.e., hours to days). Several recent studies have demonstrated that resting-state correlations can be statistically modified when preceded by continuous training on tasks that encourage the coordinated activation of specific brain areas (often in a novel pairing), and the degree of change correlates with behavioral measures of learning during the task.[123–128] Third, changes in resting-state correlations have been noted over the lifespan. For example, the development from adolescence to young adulthood is accompanied by large changes in patterns of resting-state connectivity and network organization.[117,129–132] Importantly, basic long-range anatomical connectivity is adult-like by the age of 9 months,[133] suggesting that the observed developmental changes are not due to this form of neuroanatomical change alone.

As a final alternative, changes in functional connectivity may relate to changing myelination or white matter microstructure, which continues into young adulthood[134] and may be altered with extensive training,[135] ultimately facilitating signal propagation across distant regions that might strengthen resting correlations over time. Importantly, none of the proposed sources of rs-fcMRI are necessarily mutually exclusive or exhaustive. Most likely, the observed patterns of rs-fcMRI correlations are a product of more than one mechanism.

## Final thoughts

Recent development of imaging hardware to capture brain connectivity coupled with the availability of sophisticated analysis tools to measure and understand pairwise relations has presented us with the opportunity to begin to understand the brain at the level of a complexly organized large-scale network of information processing.

If the goal is to understand how the brain is organized and behaves, then abandoning an appreciation of the biological organization of the brain can result in misrepresentations of any graphical models that have tacit assumptions necessitating accurate definition of its constituent elements. Given the current spatial resolution limit of human brain imaging, efforts should be geared toward characterizing brain areas as the objects of information processing that the nodes in a graph represent. This endeavor can be partially accomplished by capitalizing on the availability of large-scale data sets to identify "hot spots" of activity, or further development of analysis techniques that identify area boundaries or clusters based on patterns of correlation similarity, connectivity, or other referents. Similarly, edges should represent relationships between the objects of information processing (i.e., areas). Relationships can be quantified by calculating pairwise correlations of the time series of nodes wherein the strength of relationships are retained as edge weights.

Neuroscience has embraced a network-based approach as a lens under which to examine brain structure and function. Viewing the brain as a set of interacting elements whose organization is inherently complex yet ordered will undoubtedly facilitate our understanding of brain architecture, function, and its emergent behaviors across the life span, and in health and disease.

## Acknowledgments

The authors thank members of the Petersen and Schlaggar Labs for valuable discussion related to ideas in this paper. Data for figures were generously provided by Christian Beckmann, Steven Nelson, Andrew Zalesky, and Justin Vincent. Josh Siegal assisted in generating Figures 1 and 5, and Steven Nelson assisted in generating Figure 3. This work was supported by an Institute for Aging Post-doctoral Fellowship from the Canadian Institute for Health Research (GSW), HD057076 (BLS), NS61144 (SEP), and The NIH Human Connectome Project (http://www.humanconnectome.org).

## Conflicts of interest

The authors declare no conflicts of interest.

## References

1. Flourens, M.-J.-P. 1842. *Recherches Expérimentales sur les Propriétés et les Fonctions du Système Nerveux dans les Animaux Vertébrés*. J.B. Balliere. Paris.
2. Inouye, T. 1909. *Die Sehstörungen bei Schussverletzungen der kortikalen Sehsphäre nach Beobachtungen an Versundeten der letzten Japanische Kriege*. Wilhelm Engelmann. Leipzig.
3. Broca, P. 1861. Remarques sur le siège de la faculté du langage articulé; suivies d'une observation d'aphémie (perte de la parole). *Bulletins de la Société Anatomique* **6:**330–357, 398–407.

4. Wernicke, C. 1874. *Der Aphasische Symptomkomplex*. Kohn & Neigart. Breslau.
5. Fritsch, G. & E. Hitzig. 1870. Über die elektrische Erregbarkeit des Grosshirns. *Archiv für Anatomie und Physiologie*, 300–332.
6. Caton, R. 1875. The electric currents of the brain. *BMJ* **2:** 278.
7. Brodmann, K. 1909. *Vergleichende Lokalisationslehre der Großhirnrinde in ihren Prinzipien dargestellt auf Grund des Zellenbaues*. J.A. Barth. Leipzig.
8. Vogt, O. & C. Vogt. 1919. Allgemeine Ergebnisse unserer Hirnforschung. *Journal für Psychologie und Neurologie*. **25:** 273–462.
9. Petersen, S.E., P.T. Fox, M.I. Posner, *et al*. 1988. Positron emission tomographic studies of the cortical anatomy of single-word processing. *Nature* **331:** 585–589.
10. Kanwisher, N. 2010. Functional specificity in the human brain: a window into the functional architecture of the mind. *Proc. Natl. Acad. Sci. USA* **107:** 11163–11170.
11. Dejerine, J. 1892. Contribution à l'étude anatomo-pathologique et clinique des différentes variétés de cécité verbale. *Mémoires de la Société de Biologie*. **4:** 61–90.
12. Geschwind, N. 1965. Disconnexion syndromes in animals and man. I. *Brain* **88:** 237–294.
13. Posner, M.I., S.E. Petersen, P.T. Fox & M.E. Raichle. 1988. Localization of cognitive operations in the human brain. *Science* (*New York, N.Y.)* **240:** 1627–1631.
14. Friston, K. 2002. Beyond phrenology: what can neuroimaging tell us about distributed circuitry? *Ann. Rev. Neurosci*. **25:** 221–250.
15. Friston, K.J. 1994. Functional and effective connectivity in neuroimaging: a synthesis. *Human Brain Mapp*. **2:** 56–78.
16. Horwitz, B., M.A. Tagamets & A.R. McIntosh. 1999. Neural modeling, functional brain imaging, and cognition. *Trends Cogn. Sci*. **3:** 91–98.
17. Biswal, B., F.Z. Yetkin, V.M. Haughton & J.S. Hyde. 1995. Functional connectivity in the motor cortex of resting human brain using echo-planar MRI. *Magn. Reson. Med*. **34:** 537–541.
18. Prohovnik, I., K. Hakansson & J. Risberg. 1980. Observations on the functional significance of regional cerebral blood flow in "resting" normal subjects. *Neuropsychologia* **18:** 203–217.
19. Johansen-Berg, H. & M.F. Rushworth. 2009. Using diffusion imaging to study human connectional anatomy. *Ann. Rev. Neurosci*. **32:** 75–94.
20. Bressler, S.L. & V. Menon. 2010. Large-scale brain networks in cognition: emerging methods and principles. *Trends Cognit. Sci*. **14:** 277–290.
21. Bullmore, E. & O. Sporns. 2009. Complex brain networks: graph theoretical analysis of structural and functional systems. *Nat. Rev*. **10:** 186–198.
22. Power, J.D., D.A. Fair, B.L. Schlaggar & S.E. Petersen. 2010. The development of human functional brain networks. *Neuron* **67:** 735–748.
23. Greicius, M.D., B. Krasnow, A.L. Reiss & V. Menon. 2003. Functional connectivity in the resting brain: a network analysis of the default mode hypothesis. *Proc. Natl. Acad. Sci. USA* **100:** 253–258.
24. Fox, M.D. & M.E. Raichle. 2007. Spontaneous fluctuations in brain activity observed with functional magnetic resonance imaging. *Nat. Rev*. **8:** 700–711.
25. Beckmann, C.F., M. DeLuca, J.T. Devlin & S.M. Smith. 2005. Investigations into resting-state connectivity using independent component analysis. *Philos. Trans. R. Soc. Lond*. **360:** 1001–1013.
26. Damoiseaux, J.S. *et al*. 2006. Consistent resting-state networks across healthy subjects. *Proc. Natl. Acad. Sci. USA* **103:** 13848–13853.
27. Shehzad, Z. *et al*. 2009. The resting brain: unconstrained yet reliable. *Cereb. Cortex* **19:** 2209–2229.
28. Newman, M.E.J. 2010. *Networks: An Introduction*. Oxford University Press. Oxford.
29. Wasserman, S. & K. Faust. 1994. *Social Network Analysis: Methods and Applications*. Cambridge University Press. Cambridge.
30. Strogatz, S.H. 2001. Exploring complex networks. *Nature* **410:** 268–276.
31. Rosvall, M. & C.T. Bergstrom. 2007. An information-theoretic framework for resolving community structure in complex networks. *Proc. Natl. Acad. Sci. USA* **104:** 7327–7331.
32. Newman, M.E. 2006. Modularity and community structure in networks. *Proc. Natl. Acad. Sci. USA* **103:** 8577–8582.
33. Girvan, M. & M.E. Newman. 2002. Community structure in social and biological networks. *Proc. Natl. Acad. Sci. USA* **99:** 7821–7826.
34. Fox, M.D. *et al*. 2005. The human brain is intrinsically organized into dynamic, anticorrelated functional networks. *Proc. Natl. Acad. Sci. USA* **102:** 9673–9678.
35. Wig, G.S., R.L. Buckner & D.L. Schacter. 2009. Repetition priming influences distinct brain systems: evidence from task–evoked data and resting-state correlations. *J. Neurophysiol*. **101:** 2632–2648.
36. Raichle, M.E. *et al*. 2001. A default mode of brain function. *Proc. Natl. Acad. Sci. USA* **98:** 676–682.
37. Shulman, G.L. *et al*. 1997. Common blood flow changes across visual tasks: II Decreases in cerebral cortex. *J. Cogn. Neurosci*. **9:** 648–663.
38. Buckner, R.L., J.R. Andrews-Hanna & D.L. Schacter. 2008. The brain's default network: anatomy, function, and relevance to disease. *Ann. NY Acad. Sci*. **1124:** 1–38.
39. Wig, G.S. *et al*. 2008. Medial temporal lobe BOLD activity at rest predicts individual differences in memory ability in healthy young adults. *Proc. Natl. Acad. Sci. USA* **105:** 18555–18560.
40. Dosenbach, N.U. *et al*. 2006. A core system for the implementation of task sets. *Neuron* **50:** 799–812.
41. MacDonald, A.W. III J.D. Cohen, V.A. Stenger & C.S. Carter. 2000. Dissociating the role of the dorsolateral prefrontal and anterior cingulate cortex in cognitive control. *Science (New York, N.Y.)* **288:** 1835–1838.
42. Mazoyer, B. *et al*. 2001. Cortical networks for working memory and executive functions sustain the conscious resting state in man. *Brain Res. Bull*. **54:** 287–298.

43. Vincent, J.L., I. Kahn, A.Z. Snyder *et al*. 2008. Evidence for a frontoparietal control system revealed by intrinsic functional connectivity. *J. Neurophysiol*. **100:** 3328–3342.
44. Dosenbach, N.U. *et al*. 2007. Distinct brain networks for adaptive and stable task control in humans. *Proc. Natl. Acad. Sci. USA* **104:** 11073–11078.
45. Seeley, W.W. *et al*. 2007. Dissociable intrinsic connectivity networks for salience processing and executive control. *J. Neurosci*. **27:** 2349–2356.
46. McKeown, M.J. *et al*. 1998. Analysis of fMRI data by blind separation into independent spatial components. *Hum. Brain Mapp*. **6:** 160–188.
47. Greicius, M.D., G. Srivastava, A.L. Reiss & V. Menon. 2004. Default-mode network activity distinguishes Alzheimer's disease from healthy aging: evidence from functional MRI. *Proc. Natl. Acad. Sci. USA* **101:** 4637–4642.
48. Cole, D.M., S.M. Smith & C.F. Beckmann. 2010. Advances and pitfalls in the analysis and interpretation of resting-state FMRI data. *Front. Syst. Neurosci*. **4:** 8.
49. Butts, C.T. 2009. Revisiting the foundations of network analysis. *Science (New York, N.Y.)* **325:** 414–416.
50. Sejnowski, T.J. & P.S. Churchland. 1989 Brain and cognition. In *Foundations of Cognitive Science*. M.I. Posner, ed.: 301–356. The MIT Press. Cambridge.
51. Felleman, D.J. & D.C. Van Essen. 1991. Distributed hierarchical processing in the primate cerebral cortex. *Cereb. Cortex* **1:** 1–47.
52. Mountcastle, V.B. 1982. An organizing principle for cerebral function: the unit module and the distributed system. In *The Mindful Brain*. G.M. Edelman & V.B. Mountcastle, Eds.: 7–50. The MIT Press. Cambridge.
53. Sanides, F. & H. Vitzhum. 1965. Zur Architectonik der menschlichen Sehrinde und den Prinzipien ihrer Entwicklung. *Deutsche Zeitschrift fur Nervenheilkunde*. **187:** 680–707.
54. Gennari, F. 1782. *Francisci Gennari Parmensis Medicinae Doctoris Collegiati de Peculiari Structura Cerebri Nonnullisque Eius Morbis-Paucae Aliae Anatom. Observat. Accedunt*. Regio Typographeo. Parma, Italy.
55. De Valois, R.L., D.G. Albrecht & L.G. Thorell. 1982. Spatial frequency selectivity of cells in macaque visual cortex. *Vis. Res*. **22:** 545–559.
56. Hubel, D.H. & T.N. Wiesel. 1968. Receptive fields and functional architecture of monkey striate cortex. *J. Physiol*. **195:** 215–243.
57. Poggio, G.F. & B. Fischer. 1977. Binocular interaction and depth sensitivity in striate and prestriate cortex of behaving rhesus monkey. *J. Neurophysiol*. **40:** 1392–1405.
58. Schiller, P.H., B.L. Finlay & S.F. Volman. 1976. Quantitative studies of single-cell properties in monkey striate cortex. III. Spatial frequency. *J. Neurophysiol*. **39:** 1334–1351.
59. Schiller, P.H., B.L. Finlay & S.F. Volman. 1976. Quantitative studies of single-cell properties in monkey striate cortex. II. Orientation specificity and ocular dominance. *J. Neurophysiol*. **39:** 1320–1333.
60. Schiller, P.H., B.L. Finlay & S.F. Volman. 1976. Quantitative studies of single-cell properties in monkey striate cortex. I. Spatiotemporal organization of receptive fields. *J. Neurophysiol*. **39:** 1288–1319.
61. Peterhans, E. & R. von der Heydt. 1989. Mechanisms of contour perception in monkey visual cortex. II. Contours bridging gaps. *J. Neurosci*. **9:** 1749–1763.
62. von der Heydt, R. & E. Peterhans. 1989. Mechanisms of contour perception in monkey visual cortex. I. Lines of pattern discontinuity. *J. Neurosci*. **9:** 1731–1748.
63. Galaburda, A.M. & D.N. Pandya. 1983. The intrinsic architectonic and connectional organization of the superior temporal region of the rhesus monkey. *J. Comp. Neurol*. **221:** 169–184.
64. Carmichael, S.T. & J.L. Price. 1994. Architectonic subdivision of the orbital and medial prefrontal cortex in the macaque monkey. *J. Comp. Neurol*. **346:** 366–402.
65. Carmichael, S.T. & J.L. Price. 1996. Connectional networks within the orbital and medial prefrontal cortex of macaque monkeys. *J. Comp. Neurol*. **371:** 179–207.
66. Toga, A.W., P.M. Thompson, S. Mori, *et al*. 2006. Towards multimodal atlases of the human brain. *Nat. Rev*. **7:** 952–966.
67. Johansen-Berg, H. *et al*. 2004. Changes in connectivity profiles define functionally distinct regions in human medial frontal cortex. *Proc. Natl. Acad. Sci. USA* **101:** 13335–13340.
68. Johansen-Berg, H. *et al*. 2005. Functional-anatomical validation and individual variation of diffusion tractography-based segmentation of the human thalamus. *Cereb. Cortex* **15:** 31–39.
69. Cohen, A.L. *et al*. 2008. Defining functional areas in individual human brains using resting functional connectivity MRI. *NeuroImage* **41:** 45–57.
70. Nelson, S.M. *et al*. 2010. A parcellation scheme for human left lateral parietal cortex. *Neuron* **67:** 156–170.
71. Uddin, L.Q. *et al*. 2010. Dissociable connectivity within human angular gyrus and intraparietal sulcus: evidence from functional and structural connectivity. *Cereb. Cortex* **20:** 2636–2646.
72. Caspers, S. *et al*. 2008. The human inferior parietal lobule in stereotaxic space. *Brain Structure & Function* **212:** 481–495.
73. Caspers, S. *et al*. 2006. The human inferior parietal cortex: cytoarchitectonic parcellation and interindividual variability. *NeuroImage* **33:** 430–448.
74. Mumford, J.A. *et al*. 2010. Detecting network modules in fMRI time series: a weighted network analysis approach. *NeuroImage* **52:** 1465–1476.
75. Tomasi, D. & N.D. Volkow. 2010. Functional connectivity density mapping. *Proc. Natl. Acad. Sci. USA* **107:** 9885–9890.
76. Zhang, D. *et al*. 2008. Intrinsic functional relations between human cerebral cortex and thalamus. *J. Neurophysiol*. **100:** 1740–1748.
77. Barnes, K.A. *et al*. 2010. Identifying basal ganglia divisions in individuals using resting-state functional connectivity MRI. *Front. Syst. Neurosci*. **4:** 18.
78. Fischl, B. *et al*. 2004. Sequence-independent segmentation of magnetic resonance images. *NeuroImage* **23**(Suppl. 1): S69–S84.
79. Maldjian, J.A., P.J. Laurienti, R.A. Kraft & J.H. Burdette. 2003. An automated method for neuroanatomic and

cytoarchitectonic atlas-based interrogation of fMRI data sets. *NeuroImage* **19:** 1233–1239.
80. Tzourio-Mazoyer, N. *et al*. 2002. Automated anatomical labeling of activations in SPM using a macroscopic anatomical parcellation of the MNI MRI single-subject brain. *NeuroImage* **15:** 273–289.
81. Thompson, P.M., C. Schwartz, R.T. Lin, *et al*. 1996. Three-dimensional statistical analysis of sulcal variability in the human brain. *J. Neurosci.* **16:** 4261–4274.
82. Clarke, S. & J. Miklossy. 1990. Occipital cortex in man: organization of callosal connections, related myelo- and cytoarchitecture, and putative boundaries of functional visual areas. *J. Comp. Neurol*. **298:** 188–214.
83. Van Essen, D.C., W.T. Newsome, J.H. Maunsell, & J.L. Bixby. 1986. The projections from striate cortex (V1) to areas V2 and V3 in the macaque monkey: asymmetries, areal boundaries, and patchy connections. *J. Comp. Neurol.* **244:** 451–480.
84. Dougherty, R.F. *et al*. 2003. Visual field representations and locations of visual areas V1/2/3 in human visual cortex. *J. Vis.* **3:** 586–598.
85. Van Essen, D.C., J.H. Maunsell & J.L. Bixby. 1981. The middle temporal visual area in the macaque: myeloarchitecture, connections, functional properties and topographic organization. *J. Comp. Neurol*. **199:** 293–326.
86. Zalesky, A. *et al*. 2010. Whole-brain anatomical networks: does the choice of nodes matter? *NeuroImage* **50:** 970–983.
87. Fornito, A., A. Zalesky & E.T. Bullmore. 2010. Network scaling effects in graph analytic studies of human resting-state FMRI data. *Front. Syst. Neurosci.* **4:** 22.
88. Hayasaka, S. & P.J. Laurienti. 2010. Comparison of characteristics between region-and voxel-based network analyses in resting-state fMRI data. *NeuroImage* **50:** 499–508.
89. Wang, J. *et al*. 2009. Parcellation-dependent small-world brain functional networks: a resting-state fMRI study. *Hum. Brain Mapp*. **30:** 1511–1523.
90. He, B.J., A.Z. Snyder, J.M. Zempel *et al*. 2008. Electrophysiological correlates of the brain's intrinsic large-scale functional architecture. *Proc. Natl. Acad. Sci. USA* **105:** 16039–16044.
91. Nir, Y. *et al*. 2008. Interhemispheric correlations of slow spontaneous neuronal fluctuations revealed in human sensory cortex. *Nat. Neurosci.* **11:** 1100–1108.
92. Thirion, B., S. Dodel & J.B. Poline. 2006. Detection of signal synchronizations in resting-state fMRI datasets. *NeuroImage* **29:** 321–327.
93. Bullmore, E. *et al*. 2004. Wavelets and functional magnetic resonance imaging of the human brain. *NeuroImage* **23**(Suppl. 1): S234–S249.
94. Granger, C.W.J. 1969. Investigating causal relations by econometric models and cross-spectral methods. *Econometrica* **37:** 424–438.
95. Smith, S.M. *et al*. 2010. Network modelling methods for FMRI. *NeuroImage* **54:** 875–891.
96. Weissenbacher, A. *et al*. 2009. Correlations and anticorrelations in resting-state functional connectivity MRI: a quantitative comparison of preprocessing strategies. *NeuroImage* **47:** 1408–1416.
97. Murphy, K., R.M. Birn, D.A. Handwerker, *et al*. 2009. The impact of global signal regression on resting state correlations: are anti-correlated networks introduced? *NeuroImage* **44:** 893–905.
98. Fox, M.D., D. Zhang, A.Z. Snyder & M.E. Raichle. 2009. The global signal and observed anticorrelated resting state brain networks. *J. Neurophysiol*. **101:** 3270–3283.
99. Mink, J.W. 1996. The basal ganglia: focused selection and inhibition of competing motor programs. *Prog. Neurobiol*. **50:** 381–425.
100. Hikosaka, O. & R.H. Wurtz. 1983. Visual and oculomotor functions of monkey substantia nigra pars reticulata. I. Relation of visual and auditory responses to saccades. *J. Neurophysiol*. **49:** 1230–1253.
101. Damoiseaux, J.S. & M.D. Greicius. 2009. Greater than the sum of its parts: a review of studies combining structural connectivity and resting-state functional connectivity. *Brain Struct. Funct*. **213:** 525–533.
102. Honey, C.J., J.P. Thivierge & O. Sporns. 2010. Can structure predict function in the human brain? *NeuroImage* **52:** 766–776.
103. Koch, M.A., D.G. Norris & M. Hund-Georgiadis. 2002. An investigation of functional and anatomical connectivity using magnetic resonance imaging. *NeuroImage* **16:** 241–250.
104. Greicius, M.D., K. Supekar, V. Menon & R.F. Dougherty. 2009. Resting-state functional connectivity reflects structural connectivity in the default mode network. *Cereb. Cortex* **19:** 72–78.
105. Hagmann, P. *et al*. 2008. Mapping the structural core of human cerebral cortex. *PLoS Biol*. **6:** e159.
106. Honey, C.J. *et al*. 2009. Predicting human resting-state functional connectivity from structural connectivity. *Proc. Natl. Acad. Sci. USA* **106:** 2035–2040.
107. Skudlarski, P. *et al*. 2008. Measuring brain connectivity: diffusion tensor imaging validates resting state temporal correlations. *NeuroImage* **43:** 554–561.
108. Quigley, M. *et al*. 2003. Role of the corpus callosum in functional connectivity. *Am. J. Neuroradiol.* **24:** 208–212.
109. Johnston, J.M. *et al*. 2008. Loss of resting interhemispheric functional connectivity after complete section of the corpus callosum. *J. Neurosci.* **28:** 6453–6458.
110. Uddin, L.Q. *et al*. 2008. Residual functional connectivity in the split-brain revealed with resting-state functional MRI. *Neuroreport* **19:** 703–709.
111. Vincent, J.L. *et al*. 2007. Intrinsic functional architecture in the anaesthetized monkey brain. *Nature* **447:** 83–86.
112. Van Essen, D.C., W.T. Newsome & J.L. Bixby. 1982. The pattern of interhemispheric connections and its relationship to extrastriate visual areas in the macaque monkey. *J. Neurosci.* **2:** 265–283.
113. Horovitz, S.G. *et al*. 2008. Low frequency BOLD fluctuations during resting wakefulness and light sleep: a simultaneous EEG-fMRI study. *Hum. Brain Mapp.* **29:** 671–682.
114. Larson-Prior, L.J. *et al*. 2009. Cortical network functional connectivity in the descent to sleep. *Proc. Natl. Acad. Sci. USA* **106:** 4489–4494.

115. Greicius, M.D. *et al*. 2008. Persistent default-mode network connectivity during light sedation. *Hum. Brain Mapp.* **29:** 839–847.
116. Fransson, P. 2006. How default is the default mode of brain function? Further evidence from intrinsic BOLD signal fluctuations. *Neuropsychologia* **44:** 2836–2845.
117. Fair, D.A. *et al*. 2007. Development of distinct control networks through segregation and integration. *Proc. Natl. Acad. Sci. USA* **104:** 13507–13512.
118. Hampson, M., I.R. Olson, H.C. Leung, *et al*. 2004. Changes in functional connectivity of human MT/V5 with visual motion input. *Neuroreport* **15:** 1315–1319.
119. Fox, M.D., A.Z. Snyder, J.L. Vincent & M.E. Raichle. 2007. Intrinsic fluctuations within cortical systems account for intertrial variability in human behavior. *Neuron* **56:** 171–184.
120. Kelly, A.M., L.Q. Uddin, B.B. Biswal, *et al*. 2008. Competition between functional brain networks mediates behavioral variability. *NeuroImage* **39:** 527–537.
121. Monto, S., S. Palva, J. Voipio & J.M. Palva. 2008. Very slow EEG fluctuations predict the dynamics of stimulus detection and oscillation amplitudes in humans. *J. Neurosci*. **28:** 8268–8272.
122. Smith, S.M. *et al*. 2009. Correspondence of the brain's functional architecture during activation and rest. *Proc. Natl. Acad. Sci. USA* **106:** 13040–13045.
123. Albert, N.B., E.M. Robertson & R.C. Miall. 2009. The resting human brain and motor learning. *Curr. Biol*. **19:** 1023–1027.
124. Hasson, U., H.C. Nusbaum & S.L. Small. 2009. Task-dependent organization of brain regions active during rest. *Proc. Natl. Acad. Sci. USA* **106:** 10841–10846.
125. Lewis, C.M., A. Baldassarre, G. Committeri, *et al*. 2009. Learning sculpts the spontaneous activity of the resting human brain. *Proc. Natl. Acad. Sci. USA* **106:** 17558–17563.
126. Stevens, W.D., R.L. Buckner & D.L. Schacter. 2010. Correlated low-frequency BOLD fluctuations in the resting human brain are modulated by recent experience in category-preferential visual regions. *Cereb. Cortex* **20:** 1997–2006.
127. Tambini, A., N. Ketz & L. Davachi. 2010. Enhanced brain correlations during rest are related to memory for recent experiences. *Neuron* **65:** 280–290.
128. Waites, A.B., A. Stanislavsky, D.F. Abbott & G.D. Jackson. 2005. Effect of prior cognitive state on resting state networks measured with functional connectivity. *Hum. Brain Mapp*. **24:** 59–68.
129. Dosenbach, N.U. *et al*. 2010. Prediction of individual brain maturity using fMRI. *Science (New York, N.Y.)* **329:** 1358–1361.
130. Fair, D.A. *et al*. 2008. The maturing architecture of the brain's default network. *Proc. Natl. Acad. Sci. USA* **105:** 4028–4032.
131. Fair, D.A. *et al*. 2009. Functional brain networks develop from a "local to distributed" organization. *PLoS Computat. Biol*. **5:** e1000381 .
132. Supekar, K., M. Musen & V. Menon. 2009. Development of large-scale functional brain networks in children. *PLoS Biol*. **7:** e1000157 .
133. Conel, J.L. *The Postnatal Development of the Human Cerebral Cortex*: 1939–1963. Harvard University Press. Cambridge.
134. Giedd, J.N. *et al*. 1999. Brain development during childhood and adolescence: a longitudinal MRI study. *Nat. Neurosci*. **2:** 861–863.
135. Scholz, J., M.C. Klein, T.E. Behrens & H. Johansen-Berg. 2009. Training induces changes in white-matter architecture. *Nat. Neurosci*. **12:** 1370–1371.
136. Watts, D.J. & S.H. Strogatz. 1998. Collective dynamics of 'small-world' networks. *Nature* **393:** 440–442.
137. Humphries, M.D., K. Gurney & T.J. Prescott. 2006. The brainstem reticular formation is a small-world, not scale-free, network. *Proc. Biol. Sci.* **273:** 503–511.